12th International Conference on Fracture Mechanics of Concrete and Concrete Structures
FraMCoS-12
B.L.A. Pichler, Ch. Hellmich, P. Preinstorfer (Eds)

https://doi.org/10.21012/FC12.1146
TT-C2:4

NUMERICAL INVESTIGATION OF THE SHEAR BEHAVIOR OF REINFORCED CONCRETE BEAMS WITH LOW SHEAR REINFORCEMENT UNDER DIFFERENT BOUNDARY AND LOADING CONDITIONS

YASAR H. GEDIK AND NGUYEN D. TUNG

Helmut Schmidt University/University of the Federal Armed Forces Hamburg, Chair of Structural Concrete
Holstenhofweg 85, 22043 Hamburg, Germany
e-mail: gediky@hsu-hh.de, nguyend@hsu-hh.de

Key words: Reinforced concrete beams, nonlinear finite element analysis, low shear reinforcement, support condition, load arrangement, shear behavior

Abstract: The significant influence of boundary and loading conditions on the shear response of slender reinforced concrete beams without shear reinforcement has been substantiated by recent research. It would be of interest to examine whether this influence is also present in the case of beams with low shear reinforcement less than the minimum shear reinforcement ratio. This study presents a numerical investigation of the shear behavior of slender reinforced concrete beams with low shear reinforcement under various boundary and loading conditions. An experimental study from the literature is considered, comprising three beam series types: four simply supported beams subjected to a point load, three simply supported beams subjected to a distributed load, and four cantilevers subjected to a distributed load. The GID and ATENA software are utilized for 3D modeling and nonlinear finite element analysis. A novel approach to modelling distributed loads is proposed. By evaluating load-displacement curves, nominal shear stresses and shear transfer actions along the shear cracks, the influence of loading and support conditions on the shear behavior of slender reinforced concrete beams with low amounts of shear reinforcement is investigated. Due to boundary and loading conditions, normalized nominal shear stress increases up to 124%. The benefit of numerical modeling is leveraged to perform a sensitivity analysis of varying shear reinforcement locations on the shear resistance of specimens.

1 INTRODUCTION

Over the past decades, the shear failure of reinforced concrete (RC) beams without shear reinforcement has been the subject of extensive investigation in the literature [1], with the majority of test data pertaining to simply supported beams subjected to one or two-point loading. However, the presentation of the shear force diagram of such beams in practice is infrequent. On the other hand, the literature on simply supported beams and cantilevers subjected to a distributed load is limited [2-3].

To differentiate the shear behavior of RC members corresponding to various support and loading conditions, resulting in the different moment/shear force (M/V) combinations encountered in practice, it is possible to classify RC members into one of three shear span types:
-Type 1 (T1)- Shear span with constant shear force: simply supported beams or cantilevers subjected to point loading.
-Type 2 (T2): Shear span with inverse variations of shear force and bending moment: simply supported beams subjected to distributed loading or the span between zero moment points in continuous systems.
-Type 3 (T3): Shear span with coincident change of shear force and bending moment: cantilevers subjected to distributed loading.

The influence of support and loading conditions on the shear resistance of RC beams without shear reinforcement has been

previously established in recent studies. Caldentey et al. [3] demonstrated that the load capacity of a cantilever subjected to a distributed load (T3) is higher than that of a cantilever subjected to a point load (T1). Tung and Tue [2] observed that the shear resistance of types 2 and 3 specimens is higher compared to type 1 with similar cross-sectional parameters. These findings contrast with [4-5], where the negative effect of axial strain on the shear resistance is considered.

On the other hand, the design codes [6-7] stipulate the necessity for a minimum amount of shear reinforcement to prevent brittle failure of RC members without shear reinforcement. Recent experimental studies [8-10] have examined the effect of low amounts of shear reinforcement less than the minimum ($\rho_w < \rho_{w,min}$), where ρ_w is the shear reinforcement ratio and $\rho_{w,min}$ is the minimum shear reinforcement ratio, on the shear capacity of RC beams. The findings revealed that a low amount of shear reinforcement has no significant effect on the shear resistance of type 1 beams. However, the contribution to the shear resistance of type 3 beams is notable. This suggests that the support and loading conditions exert an influence on the shear resistance of RC beams. Nevertheless, such studies are scarce, and further investigations are essential to capture a more comprehensive understanding of this topic. In the absence of sufficient experimental research and reliable analytical models, numerical analysis can serve as a valuable tool to enhance our understanding of this phenomenon.

Nonlinear finite element analysis (NLFEA) has been employed extensively for decades to investigate the shear behavior of concrete members. Several aspects of the shear behavior of RC members with various cross-section types have been investigated using NLFEA to date [11-15]. The shear crack growth is examined by FEA in [16-17], which is a crucial aspect of shear behavior. However, like the tests, most numerical investigations conducted in the literature pertain to type 1 beams, and numerical studies on type 2 and 3 beams are rare, where the modeling of distributed loading is essential. This presents a significant challenge in numerical modeling when the displacement control method (DCM) is employed. To address this challenge a laborious approach was proposed in [18]. Gedik et al. [19] employed 2D NLFEA to examine the shear resistance of RC beams without shear reinforcement across three distinct shear span types. Nevertheless, the effect of a low shear reinforcement ratio ($\rho_w < \rho_{w,min}$) on the shear behavior of reinforced concrete beams under diverse loading and support conditions has not yet been the subject of numerical investigation.

This study investigates the shear behavior of slender RC beams with low shear reinforcement ($\rho_w < \rho_{w,min}$) due to various support and loading conditions using 3D NLFEA. From the experimental evidence presented by Tue et al. [20], four simply supported beams subjected to a two-point load (T1), three simply supported beams subjected to a uniformly distributed load (T2), and four cantilevers subjected to a uniformly distributed load (T3) were considered. A novel approach to modeling distributed loads in 3D, coupled with a DCM, is proposed. The load-displacement curves and nominal shear stress of beams are evaluated, and the shear transfer mechanism along the shear crack for beams with low shear reinforcement is assessed. The effect of support and loading conditions on the shear resistance of beams with low shear reinforcement is elucidated. Furthermore, the influence of shear reinforcement locations on the shear resistance of such beams is investigated through a sensitivity analysis leveraging the advantage of numerical modeling.

2 TEST PROGRAM

Eleven RC beams with rectangular cross-sections tested by Tue et al. [20] are considered, and numerically investigated.

Table 1. Classification of beams

Type	Series	Static system	Loding type
T1	S11~S14	Single span beam	Concentrated load
T2	S21~24	Single span beam	Distributed load
T3	S28~S29	Cantilever	Distributed load

The specimens are classified into three shear span types, as described in Table 1, comprising four simply supported beams subjected to a two-point load (T1), three simply supported beams subjected to a uniformly distributed load (T2), and four cantilevers subjected to a uniformly distributed load (T3).

2.1 Description of specimens

Figure 1 and Table 2 illustrate the geometric configuration and mechanical properties of specimens. A total of 18 shear tests were conducted by testing both shear span sides of simply supported beams separately. Two shear span side of those specimens are represented as "a" and "b" as indicated in Figure 1. The nomenclature used for the specimens is shown in Figure 1. To illustrate, specimens S14T1R0.7-a and S14T1R1.4-b represent two shear spans (a and b) of specimen S14, which belong to shear span type 1 (T1) and possess lower ($\rho_w / \rho_{w,min} = 0.7$) and higher ($\rho_w / \rho_{w,min} = 1.4$) shear reinforcement ratios, respectively. All specimens are classified as slender beams with a height of 450 mm. The $\rho_w / \rho_{w,min}$ ratio ranges from 0 to 1.43 for T1, 0.63 to 1.61 for T2, and 0.62 to 0.82 for T3 specimens. The load was applied using the hydraulic jack with the deformation control method. The uniformly distributed load was created through a fire hose filled with water as described in [2,21].

2.2 Test Results

The maximum machine load (P_{max}) and the shear force at d from the support ($V_{exp,d}$), including loading equipment and self-weight, are presented in Table 2. Except for specimen S14T1R1.4-b, which exhibited bending failure, all specimens failed in shear. No test results of specimens S13T1R1.4-b, S22T2R1.0-a and S24T2R1.1-a are available.

The shear resistance ($V_{exp,d}$) ranges from 65.16 kN to 92.12 kN in specimens of type 1, from 205.96 kN to 250.67 kN in specimens of type 2, and from 177.00 to 219.28 kN in specimens of type 3. A low amount of shear reinforcement ($\rho_w < \rho_{w,min}$) has no notable influence on the shear resistance of type 1 specimens, whereas this contribution is significant for type 2 and 3 specimens. That implies a remarkable impact of loading and support conditions on the shear resistance of RC beams with similar cross-sections. Further descriptions of tested specimens and results can be found in [20].

3 FE MODELING AND NUMERICAL ANALYSIS

The GID v.15 software [22] is used for 3D numerical modeling, while the nonlinear finite element analyses are conducted through ATENA Studio V.5.9 software [23]. Half 3D models are established for specimens in types 1 (S11 to S14) and 2 (S21 to S24) to simulate each side of simply supported beams (Figure 2). To reduce the computational burden, the elastic material is employed for the parts between the intermediate and top support of the cantilevers in type 3 (S28 and S29). Hexahedral elements are utilized for concrete, while 1D truss elements for reinforcement are employed. The mesh size is 30 mm. The nonlinear analysis is conducted using the Newton-Raphson method along with the DCM.

The application of the DCM in the modeling of distributed loads represents a significant challenge in structural modeling and numerical analysis. Figure 3 demonstrates a direct yet burdensome modeling approach for the simulation of distributed loading utilizing a multi-layer framework that comprises a series of rigid beams. This approach is employed in [18]. However, due to the discontinuity of the loading plates and disparate deformation behavior of rigid beams and concrete, it would be difficult to achieve a uniform stress distribution along the loading surface of the beam. This study employs a novel and effective method to address these issues. To simulate a distributed load, a continuous load distribution layer is modeled between the concrete beam and the top steel plate, on which the prescribed displacement is applied, as shown in Figure 4.a.

This layer reflects the physical properties of the fire hose filled with water. Its mechanical properties and boundary conditions are calibrated to achieve a uniform stress distribution along the beam.

Table 2. Specimen description and summary of results [20]

Specimen	Type	f_{cm} MPa	b mm	d mm	ρ_s %	ρ_w ‰	ρ_w / $\rho_{w,min}$	$P_{FEA,max}$ kN	$P_{exp,max}$ kN	$V_{exp,d}$ kN
S11T1R0.0-a	T1	34.4	170	406	0.90	0.00	0.00	69.71	68.69	71.74
S12T1R0.0-a	T1	34.3	170	406	0.90	0.00	0.00	69.71	62.11	65.16
S13T1R0.7-a	T1	34.1	170	406	0.90	0.57	0.71	78.10	78.74	81.79
S14T1R0.7-a	T1	33.9	170	406	0.90	0.57	0.72	78.10	69.88	72.93
S11T1R1.1-b	T1	34.4	170	406	0.90	0.85	1.07	83.80	73.83	76.88
S12T1R1.1-b	T1	34.3	170	406	0.90	0.85	1.07	83.80	89.07	92.12
S13T1R1.4-b*	T1	34.1	170	406	0.90	1.14	1.43	99.10	–	–
S14T1R1.4-b†	T1	33.9	170	406	0.90	1.14	1.43	99.10	105.03	–
S21T2R0.6-a	T2	38.2	190	408	1.90	0.59	0.63	226.90	241.38	205.96
S21T2R0.8-b	T2	38.2	190	408	1.90	0.76	0.81	198.00	274.28	233.38
S22T2R1.0-a*	T2	42.0	190	405	2.48	1.02	1.03	222.50	–	–
S24T2R1.1-a*	T2	37.5	190	405	2.48	1.02	1.10	189.80	–	–
S22T2R1.5-b	T2	42.0	190	403	2.49	1.49	1.51	265.80	294.29	250.67
S24T2R1.6-b	T2	37.5	190	403	2.49	1.49	1.61	223.15	252.46	227.81
S28T3R0.6-1	T3	39.6	190	408	1.90	0.59	0.62	206.80	195.38	177.00
S28T3R0.6-2	T3	37.0	190	408	1.90	0.59	0.64	206.80	219.32	197.88
S29T3R0.8-1	T3	40.0	190	408	1.90	0.76	0.79	200.20	232.64	209.51
S29T3R0.8-2	T3	37.2	190	408	1.90	0.76	0.82	200.20	243.84	219.28

*No test results - †Bending failure

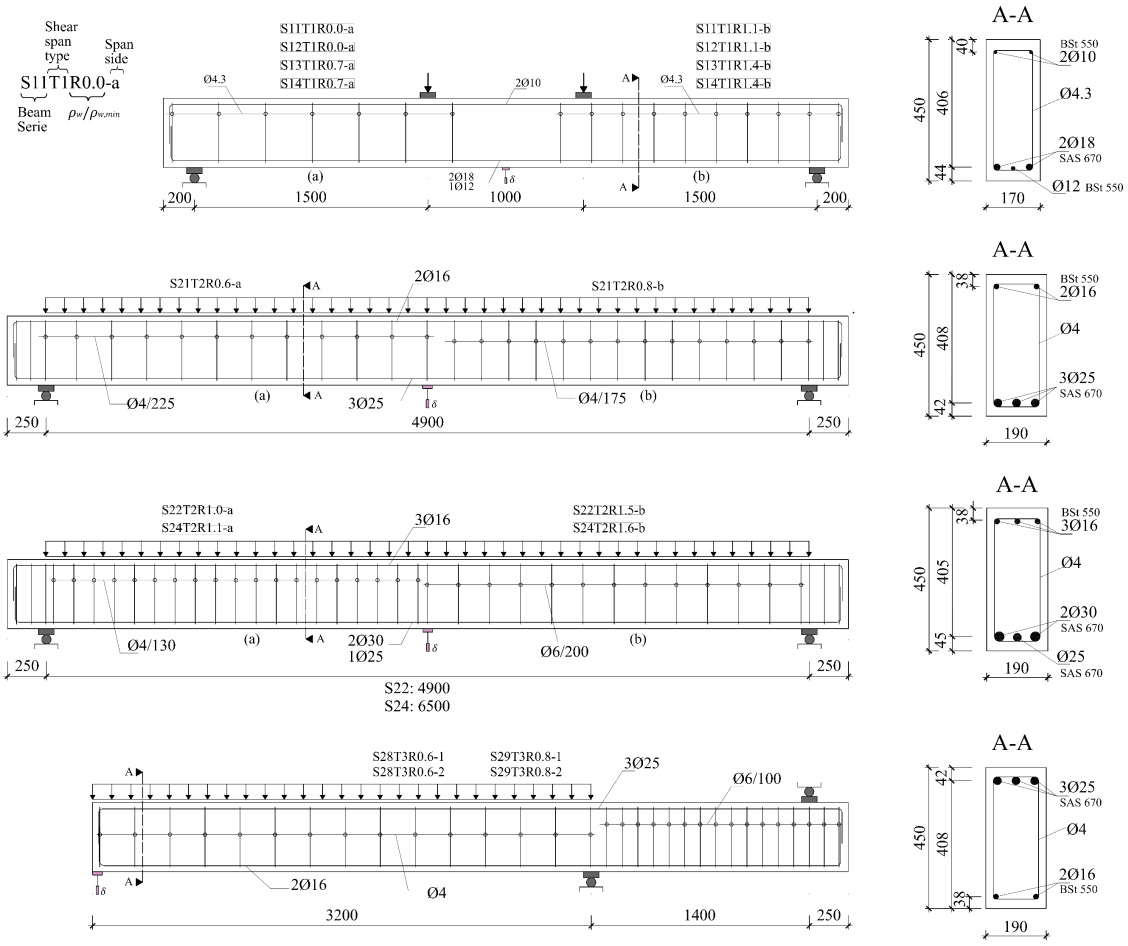

Figure 1. Specimens Overview [20]

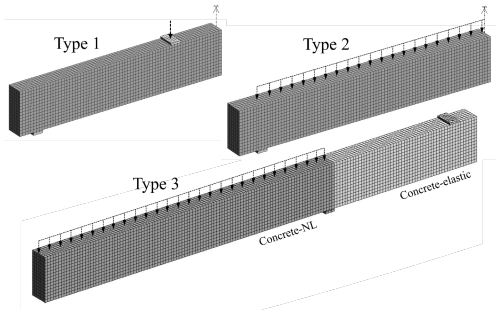

Figure 2: 3D Modeling of specimens

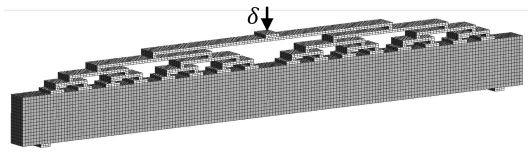

Figure 3: Multi-layer loading beams with DCM

To demonstrate the capability of the proposed method simulating uniformly distributed loading, vertical stress distribution (σ_{yy}) along the load distribution layer for the cantilever specimen S28T3R0.6 is shown in Figure 4.b. This figure depicts the stress distribution for five load levels, ranging from 20% to 100% of the peak load P_{peak}. During the loading process, the stress distribution along the load distribution layer is nearly uniform, albeit cracking initiates and propagates from the top of the cantilever, situated just beneath the distributed load. This serves to confirm the competence of the proposed method to simulate a distributed load applied through a fire hose filled with water in the test.

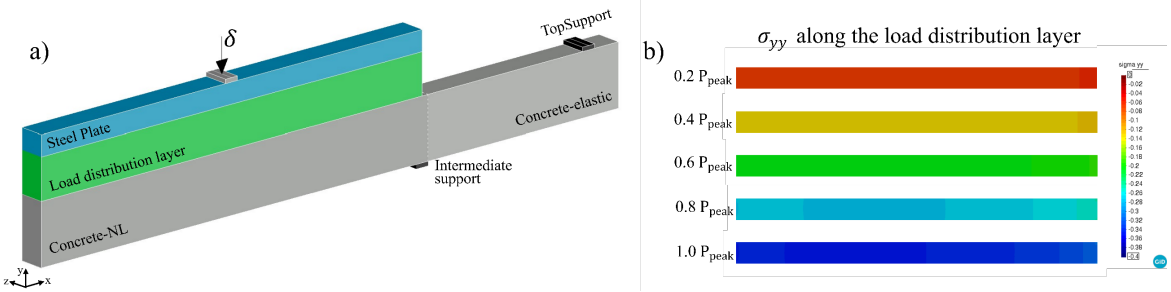

Figure 4: Modeling distributed load, a) specimen S28T3R0.6, b) vertical stress (σ_{yy}) distribution

3.1 Material modeling

The fracture-plastic constitutive model "CC3DNonLinCementitious2" for concrete included in ATENA [23] is used. This model combines compressive (plastic) behavior and tensile behavior based on nonlinear fracture mechanics. The plasticity model for concrete crushing and the Rankine fracture model for cracking are engaged. For the fracture model, the "smeared crack" formulation and the crack band model are used. The equivalent uniaxial stress-strain relationship used for concrete is shown in Figure 5. The peak stress values in tension and compression are represented by $f_t'^{ef}$ and $f_c'^{ef}$ respectively, reflecting the biaxial stress state according to [24]. The shear strength of cracked concrete is defined considering aggregate interlock as given in the MCFT [5]. The fracture energy is determined according to Hordijk [25]. The stress-strain relationship for the reinforcement is used based on EC 2 [6]. A further detailed description of the material modeling can be found elsewhere [23].

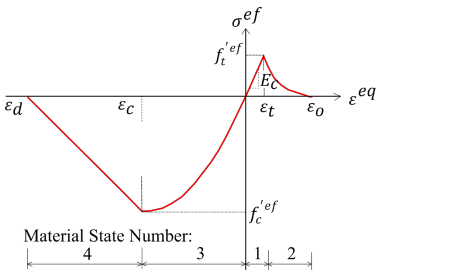

Figure 5: Uniaxial stress-strain relationship of concrete (reproduced from [23])

3.2 Numerical Results

Figure 6, 7 and 8 compare load-displacement curves between the test and FE analyses for specimens belonging to types 1, 2, and 3, respectively. A single FE model is considered for identical specimens. For example, specimen S11-12T1R0.0-a represents both the

S11T1R0.0-a and S12T1R0.0-a specimens tested. In all specimens, shear failure occurs prior to the yielding of the longitudinal reinforcement in FEA. Table 2 includes the maximum shear forces ($P_{FEA,max}$) obtained from the FEA. Four additional specimens without shear reinforcement were also generated and analyzed, namely S21T2R0.0-a, S22T2R0.0-a, S24T2R0.0-a, and S28T3R0.0, which were created to evaluate the contribution of shear reinforcement to the shear resistance of types 2 and 3 specimens. The test results of these specimens are not available.

Figure 6 illustrates the comparison of test and FEA results for type 1 specimens, demonstrating a good agreement between the test and the FEA. The increase in shear resistance due to low shear reinforcement in specimen S13-14T1R0.7-a is 12% compared to specimen S11-12T1R0.0-a without shear reinforcement. That is insignificant when the natural scatter of such beams is considered. The increases in shear resistance for specimens S11-12T1R1.1-b and S13-14T1R1.4-b are 20% and 42%, respectively, revealing that only an amount of shear reinforcement higher than the minimum makes a remarkable contribution to the shear resistance of beams in type 1.

The comparison of test and FEA results for type 2 specimens is shown in Figure 7. Compared to specimen S21T2R0.0-a without shear reinforcement, an 18% increase in the shear resistance in specimen S21T2R0.6-a with low shear reinforcement is observed. This increase for specimens with near minimum reinforcement ratio (S22T2R1.0-a and S24T2R1.1-a) is 18% and 13%, whereas those are 41% and 33%, for the specimens with shear reinforcement ratios higher than the minimum (S22T2R1.5-b and S24T2R1.6-b), respectively.

For cantilever specimens in type 3, the increase of shear resistance in specimens S28T3R0.6 and S29T3R0.8 due to a low amount of shear reinforcement is 20% and 16%, compared to specimen S28T3R0.0 without shear reinforcement (Figure 8). Compared to the specimens in type 1, type 2 and 3 specimens exhibit a higher shear resistance, indicating a significant influence of support and loading conditions.

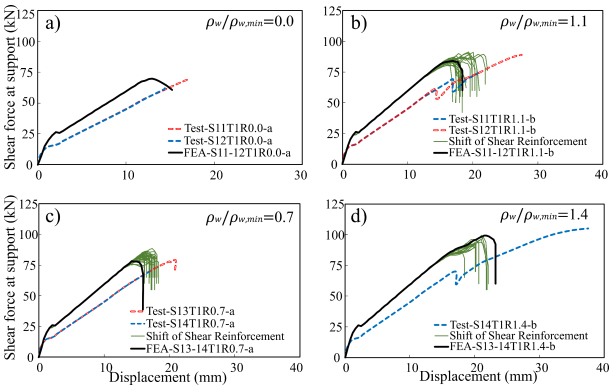

Figure 6: Comparison of load-displacement curves between test [20] and FEA for type 1

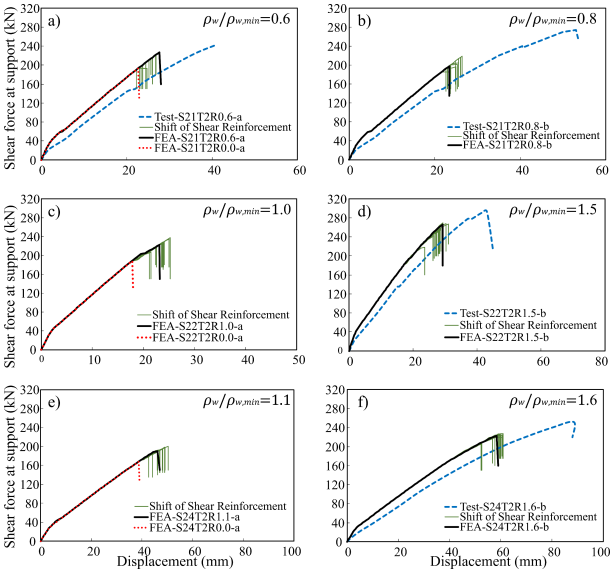

Figure 7: Comparison of load-displacement curves between test [20] and FEA for type 2

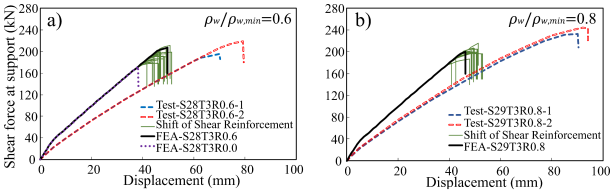

Figure 8: Comparison of load-displacement curves between test [20] and FEA for type 3

4 CONTRUBITON OF LOW SHEAR REINFORCEMENT

Through the evaluation of nominal shear stress and shear transfer analysis along the shear crack, the contribution of a low amount of shear reinforcement to the shear resistance due to loading and support conditions is numerically investigated.

4.1 Nominal Shear stress

Normalized nominal shear stress ($v_i=V_i/(b.d.\sqrt{f_c})$) of specimens is evaluated to eliminate the effect of deviation of dimensions and mechanical properties on the shear resistance. *d, V_i, b, and f_c* are the effective depth, the shear resistance at *d*, the width, and the compressive strength of concrete, respectively. The only difference remaining is the longitudinal reinforcement ratio (ρ_s). Figure 9 shows the normalized nominal shear stress (v_i) for the test and FEA for all specimens categorized into three shear span types. The specimens without shear reinforcement in the FEA are indicated as FEA-R0.0.

The normalized nominal shear stress (v_i) values of specimens of types 2 and 3 are significantly higher than those of specimens of type 1, which demonstrates the effect of the static system and loading condition on the shear resistance of RC beams. To indicate this influence more clearly, the v_i values are normalized again by the control specimen without shear reinforcement in type 1 (S11-12T1R0.0-a) and discussed.

In the FEA, the v_i values of specimen S13-14T1R0.7-a with low shear reinforcement exhibited an increase of 13% compared to specimen S11-12T1R0.0-a in type 1, which remains limited, whereas this increase is 15% in the test. The test results are given as an average v_i of corresponding identical specimens. On the other hand, the increase in the v_i values in the FEA for specimen S11-12T1R1.1-b with minimum shear reinforcement is 20%, whereas the average increase in the test is 25%. A 43% increase in the vi value of specimen S13-14T1R1.4-b with higher shear reinforcement in the FEA is obtained.

The v_i values for S21T2R0.6-a and S21T2R0.8-b specimens with low shear reinforcement in type 2 increase by 124% and 95% in the FEA, respectively, compared to the control specimens in type 1. These increases are 153% and 188% in the test.

The increase in the v_i values of cantilever specimens in type 3 due to low shear reinforcement ranges from 103% to 111% in the FEA, and 112% to 164% in the test, compared to the control specimen without shear reinforcement in type 1.

The findings illustrate a significant influence of support and loading conditions on the shear resistance of the investigated beams. The incorporation of even a low amount of shear reinforcement beneath the minimum shear reinforcement ratio has been observed to exert a considerable influence on the shear resistance of beams classified as type 2 and 3. Nevertheless, no discernible impact was observed in the case of beams in type 1.

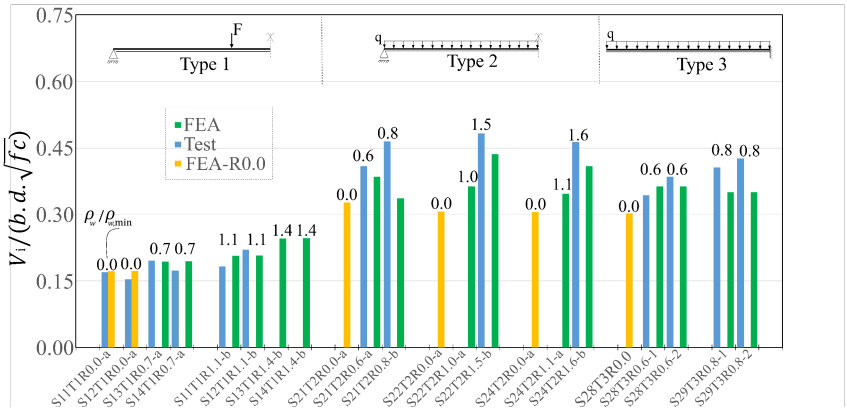

Figure 9. Comparison of nominal shear stress

4.2 Sensitivity analysis

The sensitivity analysis is carried out by FEA, generating several beam models from each specimen with shear reinforcement, to investigate the effect of shear reinforcement locations on the shear resistance of beams. In each generated beam model, the position of all shear reinforcements is shifted by 10 mm, while the spacing and shear reinforcement ratio are kept constant. The load-displacement curves

resulting from each generated specimen with shifted shear reinforcement locations are also shown in Figure 6, 7 and 8.

The impact of different shear reinforcement locations on the normalized nominal shear stress v_i is shown in Figure 10, which includes the values of the exact test configuration (v_i), the minimum ($v_{i,min}$) and maximum ($v_{i,max}$) values considering all generated beams, and their average ($v_{i,mean}$).

The disparity between the minimum ($v_{i,min}$) and maximum ($v_{i,max}$) ranges from 13% to 17% in type 1, 10% to 23% in type 2, and 19% to 20% in type 3 specimens, demonstrating a significant influence of shear reinforcement locations on the shear resistance. That might be attributed to the closeness of the shear reinforcement to the crack at the onset. If the location of the crack is close to the shear reinforcement, it can be arrested at an earlier stage and prevented from rapidly propagating, thereby enhancing the shear resistance.

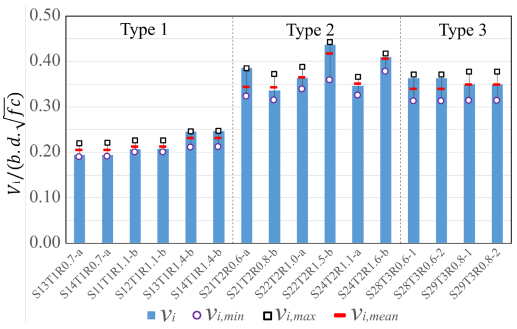

Figure 10: The effect of shear reinforcement location

specimens. The shear components are the shear resultant in the uncracked concrete (V_{cc}), the total force of shear reinforcement (V_{sw}), and the shear force carried by the cracked concrete ($V_{c,s}$), representing aggregate interlock, dowel action, and residual tensile stresses where direct shear transfer portion of the distributed load to the support for specimens S21T2R0.6-a and S28T3R0.6 is expressed by V_{direct}. The relative contribution of each shear transfer action is demonstrated in Figure 11.d.

In type 1, the direct shear reinforcement contribution (V_{sw}) is 4.4% in specimen S13-14T1R0.7-a, where the total increase in shear resistance due to a low shear reinforcement ratio is 12% compared to specimen S11-12T1R0.0-a without shear reinforcement ($V_{S13\text{-}14T1R0.7\text{-}a}$ /$V_{S11\text{-}12T1R0.0\text{-}a}$).

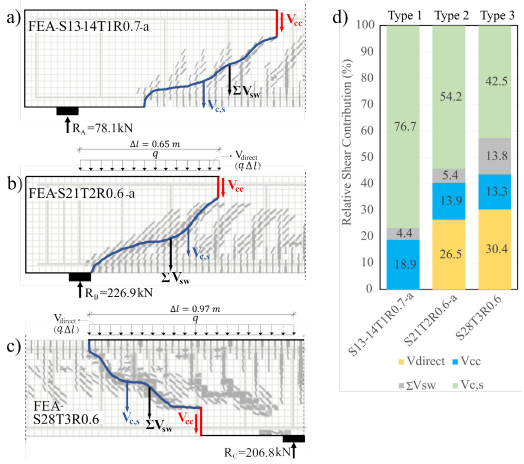

Figure 11: The analysis of shear transfer actions

4.3 Shear Transfer Analysis

The contribution of each shear transfer action to the shear resistance can be evaluated [26], by investigating the shear transfer mechanism at the shear crack. The shear transfer mechanism of specimens at the shear crack with a low amount of shear reinforcement in type 1 (S13-14T1R0.7-a), type 2 (S21T2R0.6-a), and type 3(S28T3R0.6) is investigated by FEA, to evaluate the contribution of concrete and shear reinforcement to the shear resistance. A free body (FB) equilibrium analysis is conducted on concrete elements separated by a shear crack, as shown in Figure 11.a, b, and c for three types of

The direct contribution of shear reinforcement is 5.4% for specimen S21T2R0.6-a in type 2, which remains also limited, where the total increase in shear resistance due to low shear reinforcement is 18% ($V_{S21T2R0.6\text{-}a}$ /$V_{S21T2R0.0\text{-}a}$). That might imply that even a low amount of shear reinforcement could control the cracking and provide a 13% increase in shear resistance, which could be attributed to the $V_{c,s}$ component.

This limited direct contribution of shear reinforcement (V_{sw}) could be mainly attributed to the smeared crack modeling approach used in the FEA, resulting in smaller crack widths, which is not the case in the test.

On the other hand, the direct contribution of

shear reinforcement to the shear resistance in cantilever specimen S28T3R0.6 in type 3 is 13.8%. The total increase in shear resistance is 20% ($V_{S28T3R0.6}/V_{S28T3R0.0}$), indicating the most remarkable direct shear reinforcement contribution (V_{sw}).

5 CONCLUSIONS

The effect of a low amount of shear reinforcement less than the minimum on the shear behavior of RC slender beams under various support and loading conditions is investigated numerically using NLFEA. The main conclusions can be drawn as follows:

The contribution of a low amount of shear reinforcement is limited for simply supported beams subjected to two-point loading (T1). On the other hand, this contribution is significant for simply supported and cantilever beams subjected to a distributed load (T2 and T3), which was revealed by the evaluation of the nominal shear stress.

The shift of shear reinforcement location while keeping the shear reinforcement ratio and spacing the same has a remarkable influence on the shear behavior of specimens in types 1, 2, and 3, as the early capture of a crack by a shear reinforcement prevents further crack propagation and results in higher shear resistance.

The analysis of shear components through the shear crack by FEA shows that, in type 3 specimen, the increase in shear resistance due to a low amount of shear reinforcement is mostly attributed to the direct contribution of the shear reinforcement. This increase is largely ascribed to the shear force carried by the cracked concrete in the type 2 specimens.

The different M/V combinations resulting from support and loading conditions significantly influence the shear behavior of slender RC beams with a low amount of shear reinforcement.

REFERENCES

[1] Reineck, K.H., Bentz, E.C., Fitik B., Kuchma, D.A. and Bayrak, O., 2013. ACI-DAfStb database of shear tests on slender reinforced concrete beams without stirrups. *ACI Struct. J.* **110**-5.

[2] Tung, N.D. and Tue, N. V., 2016. Effect of support condition and load arrangement on the shear response of reinforced concrete beams without transverse reinforcement. *Eng. Struct.* **111**: 370-382.

[3] Caldentey, A., Padilla, P., Muttoni, A. and Ruiz, M., 2012. Effect of Load Distribution and Variable Depth on Shear Strength of Slender Beams without Stirrups. *ACI Struct. J.* **109**-5:595-603.

[4] Muttoni, A. and Ruiz, M.F., 2008. Shear Strength of Members without Transverse Reinforcement as Function of Critical Shear Crack Width. *ACI Struct. J.* **105**-2:163-172.

[5] Vecchio, F.J. and Collins, M.P., 1986. The Modified Compression-Field Theory for reinforced concrete elements subjected to shear. *ACI J.* **88**-22: 219-231.

[6] CEN, Eurocode 2, 2010. Design of Concrete Structures - Part 1-1: General Rules for Buildings (EN 1992-1-1), Brussels: European Committee for Standardization.

[7] fib, 2013, Model Code for Concrete Structures 2010, Lausanne: International Federation for Structural Concrete.

[8] Autrup F. and Jorgensen, H.H.L., 2021. Experimental Investigation of the Shear Capacity of RC Beams with Very Small Amounts of Shear Reinforcement. *fib Symposium: New Trends for Eco-Efficiency and Performance*, Lisbon, Portugal.

[9] Tue, N. V., Betschoga, C. and Tung, N.D., 2023. Experimentelle Untersuchungen zum Einfluss des statischen Systems und der Belastungsart auf die Querkrafttragfähigkeit von Balken mit geringer Querkraftbewehrung. *Beton- und Stahlbetonbau*. **118**-7:467-477.

[10] Betschoga, C., Tung, N.D. and Tue, N. V., 2024. Influence of shear reinforcement on the shear cracking and shear resistance of simply supported beams subjected to concentrated loads and cantilevers subjected to uniformly distributed loads. Eng. Struct. 304.

[11] Slobbe, A., Hendriks; M.A.N. and Rots, J.G., 2012. Sequentially linear analysis of shear critical reinforced concrete beams without shear reinforcement. *Finite Elem. Anal. Des.* **50**:108-124.

[12] Tahenni, T., Bouziadi, F., Boulekbache, B. and Amziane, S., 2021. Experimental and nonlinear finite element analysis of shear behaviour of reinforced concrete beams. *Structures*. **29**:1582-1596.

[13] Stramandinoli, R. and Rovere, H., 2012. FE model for nonlinear analysis of reinforced concrete beams considering shear deformation. *Eng. Struct.* **35**:244-253.

[14] Huang, Z., Tu, Y., Meng, S., Bagge, N. and Nilimaa, T.B.J., 2019. Validation of a numerical method for predicting shear deformation of reinforced concrete beams. *Eng. Struct.* **197**:1-20.

[15] Demir, A., Caglar, N., Ozturk , H. and Sumer, Y., 2016. Nonlinear finite element study on the improvement of shear capacity in reinforced concrete T-Section beams by an alternative diagonal shear. *Eng. Struct.* **120**:158-165.

[16] Yang, Y., 2014. Shear behaviour of reinforced concrete members without shear reinforcement- A new look at old problem. TU Delft.

[17] Faron A. and Rombach, G., 2020. Simulation of crack growth in reinforced concrete beams using extended finite element method. Eng. Fail. Anal. **116**: 1-12.

[18] Ghahremannejad, M. and Abolmaali, A., 2018. Prediction of shear strength of reinforced concrete beams using displacement control finite element analysis. *Eng. Struct.* **169**:226-237.

[19] Gedik, Y.H., Betschoga, C., Tung, N.D. and Tue, N.V., 2023. Numerical investigation on the shear behavior of slender reinforced concrete beams without shear reinforcement differed by various boundary and loading conditions. *Structures*. **50**: 870-883.

[20] Tue, N.V., Betschoga, C. and Tung, N.D., 2019. Einfluss geringer Querkraft-bewehrung auf die Querkrafttragfähigkeit von Stahlbetonbalken unterschiedlicher M/V-Kombinationen. *Beton- und Stahlbetonbau*. **114**-4: 217-230.

[21] Leonhardt, F. and Walther, R., 1962. Schubversuche an einfeldrigen Stahlbetonbalken mit und ohne Schubbewehrung. DAfStb Heft, **151**.

[22] Riera, d.M., Tercero, E.E., Sans, A., Ribera, A., Bellart, A., Vidiella, J. and Rubio, M., 2022. GiD Reference Manual. *International Center for Numerical Methods in Engineering.* Barcelona.

[23] Červenka, V., Jendele, L. and Červenka, J., 2020. ATENA Program Documentation Part 1: Theory. *Červenka Consulting s.r.o.* Prague.

[24] Kupfer, H., Hilsdorf, H. and Rüsch, H., 1969. Behavior of Concrete under Biaxial Stress. *Journal ACI*. **66**-8:656-666.

[25] Hordijk, D., 1991. Local Approach to Fatigue of Concrete. TU Delft.

[26] Sever, Y., 2020. Numerische Untersuchung zum Effekt einer geringen Schub- bewehrung und Vorspannung auf die Querkrafttragfähigkeit von Stahlbeton- balken, Graz: TU Graz.